Electrodeposited Fe–Ga Alloy Films for Directly Coupled Noncontact Torque Sensing

Matt Hein, Jungjin Park, Joseph A. Cozzo, Alison Flatau, and Bethanie J. H. Stadler, *Senior Member, IEEE*

***Abstract*— Torque measurements are used in a number of controls applications, but indirect coupling, size, and the quality of commercially available sensor materials can limit their utility. Here, a compact magnetostrictive torque sensor is made by electrodeposition of $Fe_{1-x}Ga_x$ (0.1<x<0.4, aka Galfenol), onto Cu shafts using rotating cylinder electrodes (RCEs). The alloy composition is controlled by tuning the RCE rotation rate between 500 and 2000 RPM, while the electrode potential is varied from 1.15 to 1.20 V. Direct coupling of $Fe_{1-x}Ga_x$ to the shaft with the electrodeposition process enables magnetic anisotropy to be induced via shaft surface texturing, as seen by a 260% increase in susceptibility along a 400 grit texturing direction versus perpendicular to the texture and compared with the isotropic behavior of films deposited on polished shafts. Inverse magnetostriction-based torque sensing is demonstrated by measuring stray fields from $Fe_{1-x}Ga_x$ films as torque loads of 0–16.9 Nm were applied to the shaft. Films electrodeposited on circumferentially textured shafts had torque responses almost 1.5 times greater than films electrodeposited on longitudinally textured shafts and five times greater than films on polished shafts.**

***Index Terms*— Sensors, magnetic sensors, instrumentation and measurement, torque measurement, force sensors, thin film sensors, magnetic devices, magnetostrictive devices, magnetomechanical effects, magnetoelasticity, magnetostriction**

I. Introduction

ROTARY MOTION exists in nearly all machinery ranging from large scale windmills and diesel engines to drive shafts in cars and even to micro drills used within the vessels of human hearts. For better control of these devices, feedback is key; thus quality torque measurements are extremely important. Quality measurements are often achieved at the cost of large size and poor efficiency, so engineering tradeoffs must be made in order to get products to market. The materials and measurements presented here are an effort to introduce new solutions that offer small sensors with high efficiency and reliability. $Fe_{1-x}Ga_x$ (0.10<x<0.40, a.k.a. Galfenol), is a sensing material that exhibits saturation magnetostriction of up to 400 ppm and has saturation magnetization values of ~1.7 T. Here we use inverse magnetostriction (the Villari effect) to demonstrate that electrodeposition of $Fe_{1-x}Ga_x$ directly onto shafts enables low-power, noncontact, directly-coupled torque/strain measurements. Specifically, direct deposition of $Fe_{1-x}Ga_x$ films onto cylindrical shafts using rotating cylinder electrodes (RCE) is demonstrated for the first time, and a noncontact torque sensor is subsequently realized.

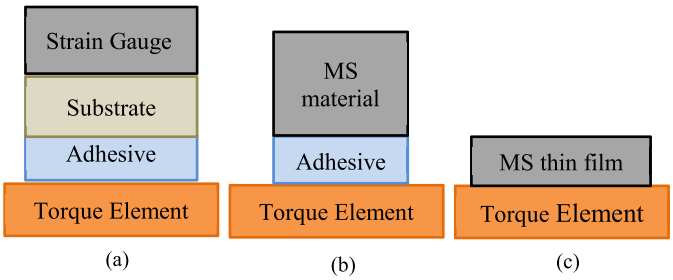

Fig. 1. a) Typical layers in strain gauge-based torque sensor. b) Bulk MS materials adhered to a torque element. c) MS thin film electroplated directly to torque element.

II. Background

A. Torque Sensors

A number of commercial technologies currently exist for torque sensing, but the sensing material rarely has direct contact with the element being strained [1], [2]. Fig. 1 shows three different styles of sensors, including a typical strain gauge (Fig. 1a) where the sensing material is grown on a specified substrate which is then adhered to the torque element [3]. The substrate, the adhesive, and alignment can all be sources of error in torque measurements. Additionally, these gauges require either direct contact via wires or slip rings, or indirect contact in which measurements are acquired via an inductive coupling resonant circuit on the shaft. Fig. 1b shows a bulk sensing material adhered directly to the torque element [4]. Using this method, the properties of the adhesive will still impact the sensed torque. Fig. 1c is an illustration of the proposed technological solution in this paper where the sensing material is deposited directly onto the element being measured. Similar solutions have been proposed in a number of patents and papers, but this is the first time the principle has been demonstrated with electrodeposited $Fe_{1-x}Ga_x$ [5]–[8]. Advantages such as facile manufacturability, good magneto-mechanical coupling, robust mechanical properties,

Manuscript received January 1, 2019; revised March 9, 2019; accepted March 11, 2019. Date of publication March 19, 2019; date of current version July 17, 2019. This work was supported by NSF under Grant ECCS-1231993. The associate editor coordinating the review of this paper and approving it for publication was Prof. Marco Petrovich. *(Corresponding author: Matt Hein.)*

M. Hein is with the Electrical and Computer Engineering Department, University of Minnesota Twin Cities, Minneapolis, MN 55455 USA (e-mail: heinx055@umn.edu).

J. Park, J. Cozzo, and A. Flatau are with the Aerospace Engineering Department, University of Maryland, College Park, MD 20742 USA (e-mail: pjj@umd.edu; valeerni@gmail.com; aflatau@umd.edu).

B. J. H. Stadler is with the Electrical and Computer Engineering Department, University of Minnesota Twin Cities, Minneapolis, MN 55455 USA, and also with the Chemical Engineering and Material Science Department, University of Minnesota Twin Cities, Minneapolis, MN 55455 USA (e-mail: stadler@umn.edu).

Digital Object Identifier 10.1109/JSEN.2019.2906062

and direct coupling make electroplated $Fe_{1-x}Ga_x$ a promising addition to the field of torque sensors.

B. Magnetostrictive (MS) Materials

For direct coupling, there are a number of magnetostrictive (MS) materials that could be considered. Terfenol-D has a large MS constant ($\lambda = 1500$ ppm), with saturation magnetization value of $B_s = \sim 1.0$ T, but the material is brittle and would be difficult to electrodeposit due to the easy oxidation of soluble rare earths, such as terbium and dysprosium [9]. Co-Fe-O ferrites have been used by many researchers for MS sensors, and single crystals have been reported to have λ as large as 400 ppm with $M_s \approx 0.6$ T [10]–[12]. However, in film form, these oxides and various other MS ferrites are typically restricted to fabrication by planar vacuum-deposition techniques. To obtain ductile, conformal depositions on a cylindrical torque element, metals such as Ni, Co, or $Fe_{1-x}Ga_x$ could be electrodeposited. Ni and Co have low MS constants ($\lambda_{Ni} \approx$- 40 ppm, $M_s = 0.6$ T; $\lambda_{Co} \approx$ -18 ppm, $M_s = 1.4$ T), but single crystal $Fe_{1-x}Ga_x$ has λ up to 400 ppm with $M_s = 1.7$ T [13], [14]. Although electrodeposited $Fe_{1-x}Ga_x$ films only have $\lambda = 100 - 200$ ppm and $M_s = 1.6$ T the truly unique capability of direct, conformal deposition onto torque elements makes them very promising as a new solution to the field of torque sensing, and a prototype device is demonstrated here [15].

C. Induced Anisotropy for Self Bias

A common design criterion in magnetic-based sensors is the need to align the primary magnetic axis of the sensor to take full advantage of the stimulus and sensing mechanisms. To do this, permanent magnets and/or electromagnets are often used, which add complexity, cost, and/or power losses [16]–[18]. Alternatively, magnetic bias can be induced by shape, coupling layers, and texture [4], [19], [20]. While these approaches can be complex, the final device can be small with all components fully integrated. For example, Herbst [6] coupled two rings with respect to each other after application of a field in order to maintain a bias direction. Raghunath *et al.* [4] used patches of textured rolled sheet with known magnetic easy axes orientations to achieve directionality. In this manuscript, a simple substrate pretexturing process is introduced so that electrodeposited $Fe_{1-x}Ga_x$ films possess a well-defined magnetic anisotropy. While this pretexturing does not relieve the need for a bias magnet in the configuration used in this paper, the induced anisotropy adds directionality to the sensor which improves its response.

D. $Fe_{1-x}Ga_x$ Electrodeposition

Electrodeposition of $Fe_{1-x}Ga_x$ was first demonstrated by McGary and then later refined and characterized by Reddy and Estrine [15], [20]–[22]. In these works, uniform, high quality films were deposited onto rotating disk electrodes (RDE), and the importance of boundary layer control was shown. To date, the electrodeposition parameters of $Fe_{1-x}Ga_x$ have only been defined for planar surfaces. In this paper, rotating cylinder electrodes (RCE) are made to elucidate the mechanisms of boundary layer control on cylinders which represent standard torque elements, such as shafts. While RDE and RCE are very similar in principle, their fluid dynamics can be very different [23]–[26]. The RDE is typically used in the laminar flow regime, which extends to very high rotation rates before becoming turbulent. The RCE on the other hand will switch from laminar to turbulent flow at very modest rotation rates.

III. Experimental Section

A. Shaft Preparation Details

In this work, two types of substrates were used: Cu tubes and Cu Shafts. To develop the electrodeposition parameters, 25.4 mm (1") diameter x 38.1 mm (1.5") long Cu tubes were cut from 152.4 mm (6') long Copper 101 tube (McMaster-Carr). After cutting, each tube was sanded with 80 grit sand paper (3M) in a circumferential direction to remove surface defects. Next, the tubes were sanded with progressively higher grits up to 400, 600, or 3000 grit. After polishing, two texture directions were created using 400 grit: circumferential and longitudinal. The Cu shafts (25.4 mm diameter by 381.0 mm (15") long) were cut from a 0.91 m (3') Copper 101 solid shaft (McMaster-Carr). A key slot was then cut on both ends to mate with the test fixture used in the prototype torque sensor. A threaded and tapped hole was also added to each end for mounting directly to the RCE motor. The shafts then followed the same surface preparation procedure as the tubes.

B. Deposition Details

In order to optimize the electrodeposition of $Fe_{1-x}Ga_x$ on cylindrical surfaces, two solutions, compositions and a variety of potentials and rotation rates were studied. The solutions were based on [21] and consisted of 500 mM sodium sulfate (Alpha Aesar), 31 mM sodium citrate (Alpha Aesar), either or 82.5 mM Gallium sulfate hydrate (Alpha Aesar), and 15 mM Iron Sulfate (Alpha Aesar). The solution PH was then adjusted to a value of 3.75 with NaOH using a calibrated PH meter (Oakton pH 6+). The potential was varied between 1.05 V and 1.25 V, using a Gamry PCI4/300. The rotation rate was controlled using a Gamry 710 RDE with rates ranging from 500 RPM up to 3200 RPM in order to mimic the RDE mass transfer rates from [21].

The Gamry RDE was replaced with a custom RCE in order to deposit onto the 381 mm shafts. Fig. 2a shows a diagram of the RCE with the two-piece shaft. The electrolytic cell consisted of a plastic 1 L graduated cylinder with two plugs machined to fit inside the cell and minimize electrolyte volume. A Ag/AgCl reference electrode (BASF) was inserted through the top plug such that it was in close proximity to the working electrode (a cylindrical shaft). The top plug also served to minimize the vortexing of the fluid during depositions. A Stainless-Steel mesh was used for the counter electrode. For the Cu tube samples, a custom fixture that mimicked a shaft was fabricated from a 25.4 mm dia. x 342.9 mm long (13.5") 7071 Al shaft that was split in two and then screwed together to hold the Cu tubes and make contact. The Al shafts were then masked to prevent deposition or corrosion. The Cu shaft samples, Fig. 2c, were simply treated as shafts

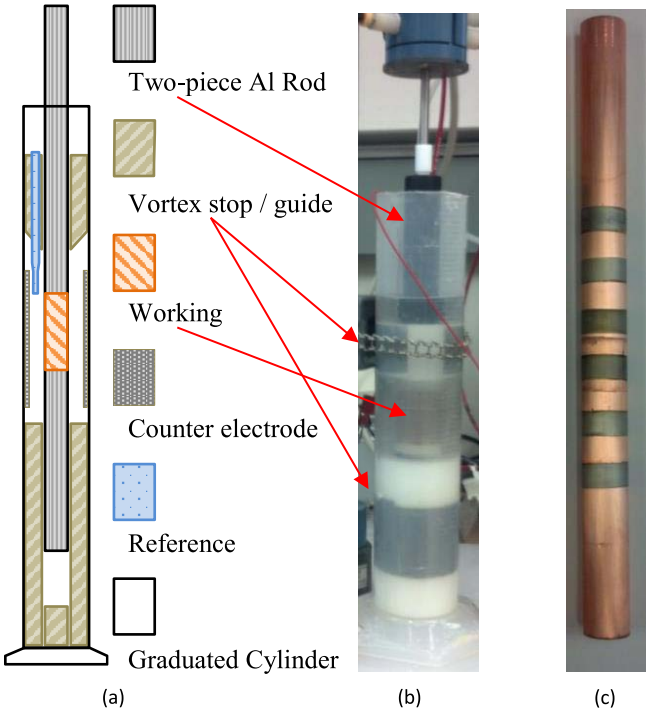

Fig. 2. a) Schematic of rotating cylinder electrode(RCE) electrodeposition cell. b) Image of RCE used in depositions, shown with two-piece shaft. c) Example of shaft with $Fe_{1-x}Ga_x$ films used for torque.

that screwed directly into the RCE motor. After deposition, the Cu shafts could be directly inserted into the torque measurement setup. During deposition both the tubes and the shafts were masked to expose a 6.35 mm (0.25") long ring of Cu to the electrolyte.

C. Measurement Details

The films were characterized by three different methods: energy dispersive spectroscopy (EDS) for composition, and vibrating sample magnetometry (VSM) for magnetic properties, and custom torque measurements for magnetostrictive response [12]. Specifically, a Jeol JSM-6610LV SEM with an Oxford Instruments Inca X-Act EDS was used to determine the %Ga, %Fe, and %O in each film, after removing peaks from Cu and trace elements. For VSM (Lakeshore 7410), 6.35 mm x 6.35 mm samples with thickness of 250 nm (estimated) were cut from the Cu tubes and mounted to a quartz rod for measurement with the magnetic field parallel to the plane of the film with the polished/textured direction both parallel to the magnetic field and rotated 90°. The magnetization was measured while the applied field was swept ±0.2 T to saturate the samples. Due to sample texture, thickness was estimated based on the film's moment. A saturation magnetization of 1520 kA/m was used as previously reported for electrodeposited samples [27].

A prototype torque sensor verified the functionality of directly coupled $Fe_{1-x}Ga_x$, Fig. 3. Films with nominal thicknesses up to 250 nm (estimated from VSM) were deposited on solid Cu shafts that had surfaces with either a polished, longitudinal or circumferential texture. The films were

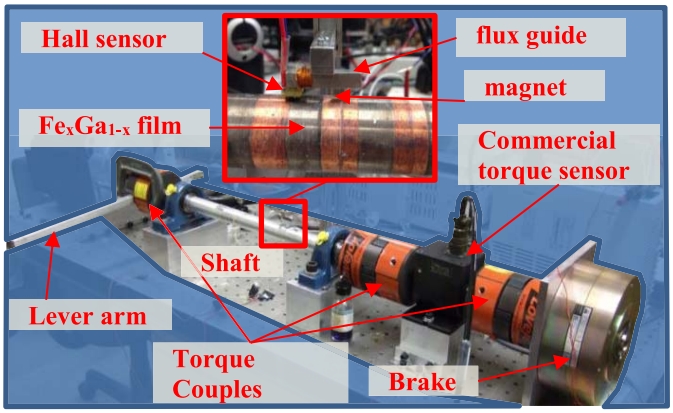

Fig. 3. Picture of torque measurement technique. The image shows testing on Al shafts with bulk foil, while the close-up shows measurement electrodeposited films [3].

deposited for 10 min at 1.2 V and 1500 rpm to achieve a composition of $Fe_{85}Ga_{15}$. The end of each Cu shaft was fixed using a particle brake (Placid Industries, Inc.). A lever arm was attached to the other end and known weights (2.27 kg (5 lb), 4.53 kg (10 lb), 6.80 kg (15 lb)) were used to apply static torque to the shaft. The weights were hung 254 mm (10") away from the shaft to create 5.65 Nm (50 in-lb), 11.30 Nm (100 in-lb), or 16.95 Nm (150 in-lb) of torque. A calibrated commercial slip ring torque sensor (Sensor Developments Inc. model 01324-022-G00A0) was used to provide standard readout of the torques for calibration. The sensor had a sensitivity of 10 mV/in-lb and a range of 0.35 Nm (3.125 in-lb) to 2300 Nm (20,000 in-lb) which covers the 5.65 Nm to 16.95 Nm range used in the experiments. Torque couples (Lovejoy inc.) were used in between each connection to ensure a reliable torque linkage. A magnetic circuit, composed of a Hall Effect sensor (AKM EQ-730L) and a biasing magnet (0.4 T) on high-permeability steel, was suspended ~1 mm above the deposited $Fe_{1-x}Ga_x$ strip on the shaft, with the air gap providing non-contact measurement. The Hall Effect sensor was oriented to sense magnetic field strength in the vertical orientation such that the sensor operated within its linear range. This circuit created a flux path through the magnet, the steel, the sensor and the $Fe_{1-x}Ga_x$ as shown in Fig 4. For each of the $Fe_{1-x}Ga_x$ films, four torque states (0, 5.65, 11.30, and 16.96 Nm) were applied to the shaft, and output was recorded simultaneously from both the Hall Effect sensor and the standard torque sensor. Sensitivity was calculated using the Hall Effect signal at each applied torque after filtering and averaging to remove noise. A least-squares regression was applied to determine the response of the sensor in μT/Nm.

When torque is applied to the shaft, torsional strain and shear stress on the surface of the shaft produce maximum tensile and compressive stresses in the $Fe_{1-x}Ga_x$ film at ±45° from the longitudinal axis of the shaft [28], [29]. The inverse magnetostrictive response of the film causes the magnetic anisotropy to align with the direction of maximum tensile stress, i.e. at an orientation of ±45° from the longitudinal axis of the shaft, so as to minimize magneto-mechanical anisotropy energy in the $Fe_{1-x}Ga_x$ film. This produces a measurable

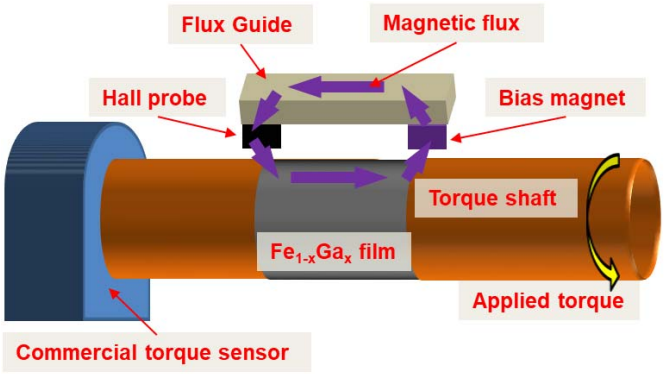

Fig. 4. Illustration of torque measurement technique.

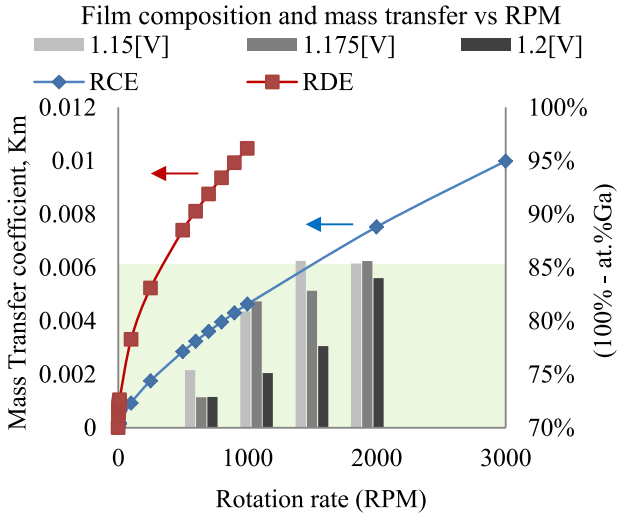

(a)

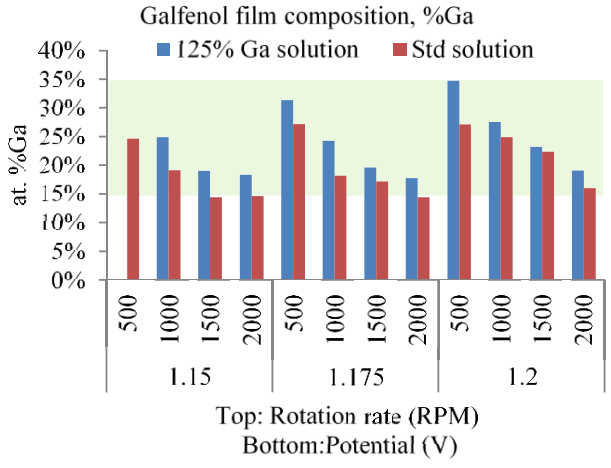

(b)

Fig. 5. a) Variation of film composition with mass transfer rate and RPM. b) %Ga content of films with various rotation rates and applied potential for the standard plating solution and the +25%Ga plating solution. Highlighted area is the range of desired composition (Ga_xFe_{1-x}, 0.15<x<0.35).

change in the magnitude of the flux passing through the magnetic circuit. The Hall effect tracks this change in the magnitude of vertical magnetic flux.

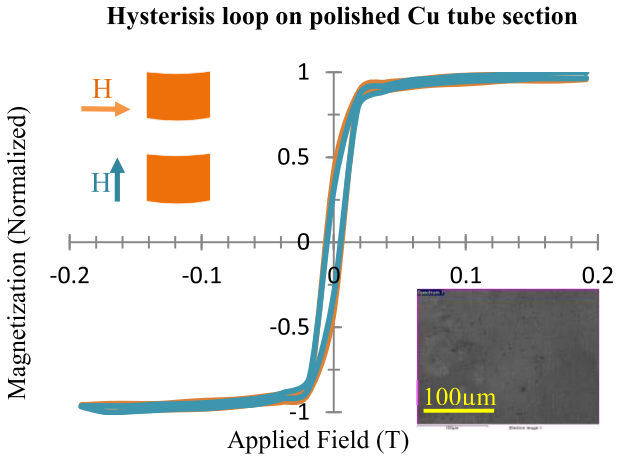

(a)

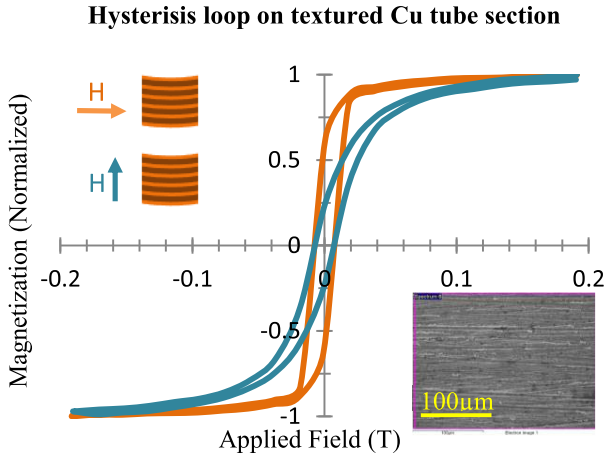

(b)

Fig. 6. a) Hysteresis loop of $Fe_{1-x}Ga_x$ film on a polished surface. b) Hysteresis loop of $Fe_{1-x}Ga_x$ film on a textured surface. Insets: SEM images of $Fe_{1-x}Ga_x$ films on polished and textured surfaces.

IV. Results

A. Rotating Cylinder Electrode vs Rotating Disk Electrode

The first step in achieving $Fe_{1-x}Ga_x$ deposition on cylinders was to modify the parameters from the RDE work of Reddy and Estrine for the RCE (Fig. 5a). Ga is typically deposited using a citrate (Cit) complexing agent. Since Fe is more electronegative than the GaCit complex, it deposits faster than Ga. So an excess of Ga is used in the electrolyte, along with controlled mixing to hone in the Ga:Fe ratio. The mass transfer (k_m) characteristics of RCE and RDE are shown in Eqs. (1) and (2) where d is the cylinder diameter, D is the diffusion coefficient, υ is kinematic viscosity and ω is rotation rate [24]

$$k_{m,RCE} = \left(0.0487 d^{0.4}\right)\left(D^{0.644}\right)\left(\upsilon^{-0.344}\right)\left(\omega^{0.7}\right) \quad (1)$$

$$k_{m,RDE} = \left(0.620 D^{\frac{2}{3}}\right)\left(\upsilon^{-\frac{1}{6}}\right)\left(\omega^{\frac{1}{2}}\right) \quad (2)$$

Calculations show that faster rotation rates are needed in RCE compared to RDE to achieve similar k_m values, Fig. 5a. For example, to match the k_m values of RDE at 1000 rpm from the prior work, 3200 rpm would be needed in RCE. However, this

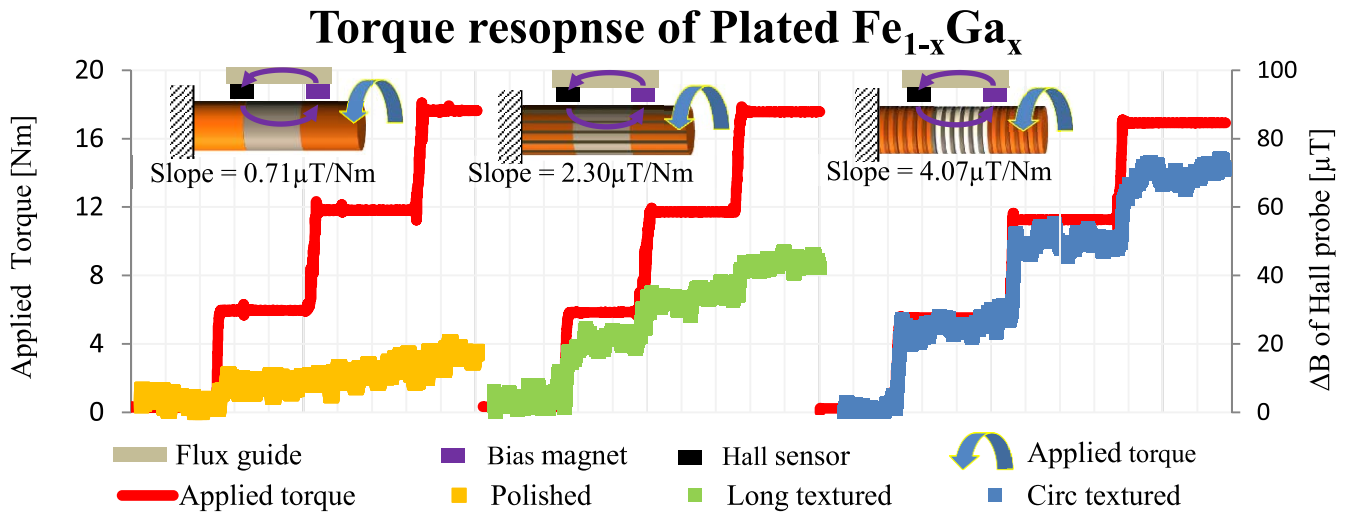

Fig. 7. Torque measurement set up and response of electroplate $Fe_{1-x}Ga_x$ films. Red, applied toque as measured by commercial torque meter. Yellow, polished shaft. Green, longitudinally textured shaft. Blue, circularly textured shaft. Insets show the magnetic circuit with the purple arrow representing the first circuits flux

rotation rate is extremely fast for RCE applications. From Eq. (3), 3200 rpm yields a Reynolds number of 106,880 which indicates high turbulence.

$$Re_{RCE} = (\pi 2 d_{cyl} F)/60\upsilon \tag{3}$$

Indeed, early attempts to match the k_m of RDE led to excessive vortex formation at the RCE's surface. The resulting turbulence led to chalky brown films typical of oxidized $Fe_{1-x}Ga_x$. The vortex stop shown in Fig. 2a was developed to limit this effect, but vortex formation was only mitigated at rotation rates below 2500 rpm. Therefore, all further development was performed using the vortex stop at rotation rates between 500 and 2000 rpm. Unfortunately, the vortex stop trapped air and bubbles in the cell, but a simple solution of relief channels, machined into the vortex stop, were effective at eliminating excessive bubble entrapment.

B. Film Composition

EDS analysis of the films showed that the Ga concentrations were indirectly proportional to the mass transfer, Fig. 5a (right axis), as expected. Fig. 5b summarizes the dependence of Ga concentration on rotation rate, deposition potential, and electrolyte concentration. This bar chart shows that the composition can be controlled over the 15%Ga to 35%Ga range that has been shown to have useful magnetostriction constants [15]. It is also important to note that the $Fe_{1-x}Ga_x$ films made within the parameters studied here did not contain oxygen impurities within the limit of detection.

C. Magnetic Characterization

The impact of substrate texture was studied using 62.5 mm^2 samples of $Fe_{1-x}Ga_x$films on polished Cu tubes (3000 grit) and textured (400grit) Cu tubes, Fig. 6a,b. The polished tube, Fig. 6a, yielded VSM loops that were almost identical in both the transverse and longitudinal measurements because the polycrystalline film was isotropic. In contrast, Fig. 6b shows that the surface of the 400 grit substrate is highly textured. The deep grooves induced a shape anisotropy in the film, which made it magnetically softer along the direction of texture. The susceptibility is 260% higher and the remanent magnetization of the textured film 2.5x greater in the direction of texturing.

D. Realization of Electroplated Torque Sensors

Prototype torque sensors were made from shafts with the three textures and torques of between 0 and 16.95 Nm were applied for measurements. The plots show the applied static torque, as recorded by a calibration torque meter, and the resulting change in magnetic flux through the magnetic circuit, as recorded by the Hall Effect sensor. As torque was applied in steps of 5.65 Nm, the calibrated torque sensor responded with a step wise increase in the output following a small transient due to the addition of weights to the lever arm. Other transients in the calibrated torque sensors are due to noise in the environment. Similarly, the Hall sensor output increased (the applied negatively signed B-field (∼12 mT,∼1.0 V) increased towards zero) with the applied torque. This increase was due to the rotation of magnetization state of the $Fe_{1-x}Ga_x$ film away from its no-load state, which was longitudinal due to biasing, towards 45° to the shaft axis.

The polished shafts showed a response of 0.71 μT/Nm. The longitudinally textured shafts showed a greater response with a sensitivity of 2.30 μT/Nm, and the circumferentially textured shafts showed the best response with a sensitivity of 4.07 μT/Nm.

The effect of texturing can be explained as a balance of stress anisotropy and shape anisotropy. The no-load magnetic anisotropy was determined by the combined effects of the shaft surface texture, the strength of the permanent magnet and flux through the torque-sensing magnetic circuit. Smooth shafts exhibited the smallest response to torque-induced stress because they had isotropic magnetization characteristics, i.e. no dominant easy axes (VSM data and Fig. 7, left). Shafts with longitudinal texture had longitudinal shape anisotropy, which is in the same direction as the no

load magnetization. In this case, (Fig. 7 middle) stress-induced anisotropy produced a modest rotation of magnetic anisotropy of the $Fe_{1-x}Ga_x$ film away from its no-load direction with a change of 2.30 μT/Nm in flux through the magnetic circuit. For circumferentially-textured shafts, the $Fe_{1-x}Ga_x$ magnetic texture-induced anisotropy lies 90° to magnetic flux path which is along the shaft. This extra circumferential anisotropy lowered the stress-anisotropy energy required to rotate the moment away from the no-load magnetically biased state. For this case (Fig. 7 right), stress-induced anisotropy produced an increase of ∼70% in rotation of magnetic anisotropy of the $Fe_{1-x}Ga_x$ film away from its no-load direction, leading to a change of 4.07 μT/Nm in flux through the magnetic circuit. Hence, this prototype sensor was more sensitive to torque within the measured range. Future sensors could control the sensitivity to different ranges of torque by varying the texture of the shaft and the strength of the permanent magnet (recall that 0.04 T permanent magnets were used here). These variables could expand the dynamic range of torques that can be detected.

For comparison to current devices, the sensitivity of the 250 nm (estimated from VSM) electrodeposited $Fe_{1-x}Ga_x$ is about 10 fold lower than the sensitivity of discrete 635 μm thick $Fe_{1-x}Ga_x$ patches, which are attached to the shafts via adhesives [30]. Further studies with thicker films are needed to determine the extent to which electrodeposited films can compete with adhesively bonded patches. Electrodeposited $Fe_{1-x}Ga_x$ films may be the only option when nano- or micro-scale torque sensors are needed, and this work verifies that they will be viable options.

V. Conclusion

Direct deposition of magnetostrictive $Fe_{1-x}Ga_x$ has been demonstrated onto torque elements using a rotating cylinder electrode (RCE) for use in torque sensors. By varying the RCE rotation rate (500-2000 rpm), deposition potential (1.0-1.2 V), and electrolyte, the film composition was controlled from 15%Ga to 35%Ga which is the optimal range for magnetostriction in the $Fe_{1-x}Ga_x$ alloy system. Additionally, it was shown that texturing the surface onto which the film was deposited affected the film's response by inducing a magnetic anisotropy. The advantages of these torque sensors are that they are easy to fabricate, allow for direct coupling, and are noncontact. With sensitivities in the range of 0.70 to 4.07 μT/Nm, these sensors are promising new directly-integrated alternatives for future applications.

VI. Acknowledgements

Parts of this work were carried out in the Characterization Facility, University of Minnesota, which receives partial support from NSF through the MRSEC program. Additionally the UMN NFC with the support of the NNIN for their facilities and technical assistance.

References

[1] R. Schicker, G Wegener. *Measuring-Torque-Correctly*. Acessed: Feb. 11, 2018. [Online]. Available: https://www.hbm.com/fileadmin/mediapool/files/torque-book/HBM_Measuring-Torque-Correctly_COMPLETE-EDITION.pdf

[2] A. S. Morris and R. Langari, *Measurement and Instrumentation: Theory and Application*, 2nd ed. London, U.K.: Academic, 2016. [Online]. Available: http://www.sciencedirect.com/science/article/pii/B9780128008843000186

[3] Micro-Measurements. (May 2018). *Strain Gage Selection: Criteria, Procedures, Recommendations*. Vishay Precision Group Micro-Measurements, Wendell, NC, USA. [Online]. Available: http://www.vishaypg.com/docs/11055/tn505.pdf

[4] G. Raghunath, A. B. Flatau, A. Purekar, and J.-H. Yoo, "Non-contact torque measurement using magnetostrictive galfenol," in *Proc. ASME Conf. Smart Mater., Adapt. Struct. Intell. Syst.*, Snowbird, UT, USA, 2013, p. V001T04A013.

[5] T. Sugihara, K. Yoshida, K. Inoue, J.-B. Yang, and I. Suzuki, "Shaft having a magnetostrictive torque sensor and a method for making same," U.S. Patent 5 585 574, Dec. 17, 1996.

[6] J. F. Herbst, "Collarless circularly magnetized torque transducer and method for measuring torque using the same," U.S. Patent 6553847B2, Apr. 29, 2003.

[7] I. J. Garshelis and C. R. Conto, "A magnetoelastic torque transducer utilizing a ring divided into two oppositely polarized circumferential regions," *J. Appl. Phys.*, vol. 79, no. 8, p. 4756, 1996.

[8] G. S. N. Rao, O. F. Caltun, K. H. Rao, P. S. V. S. Rao, and B. P. Rao, "Improved magnetostrictive properties of Co–Mn ferrites for automobile torque sensor applications," *J. Magn. Magn. Mater.*, vol. 341, pp. 60–64, Sep. 2013.

[9] Geoffrey P. McKnight and Gregory Paul Carman, "Large magnetostriction in Terfenol-D particulate composites with preferred [112] orientation," vol. 4333, pp. 178–184, Jul. 2001. doi: 10.1117/12.432754.

[10] P. N. Anantharamaiah and P. A. Joy, "High magnetostriction parameters of sintered and magnetic field annealed Ga-substituted $CoFe_2O_4$," *Mater. Lett.*, vol. 192, pp. 169–172, Apr. 2017.

[11] S. Liang, B. G. Ravi, S. Sampath, and R. J. Gambino, "Atmospheric plasma sprayed cobalt ferrite coatings for magnetostrictive sensor applications," *IEEE Trans. Magn.*, vol. 43, no. 6, pp. 2391–2393, Jun. 2007.

[12] Y. Chen, J. E. Snyder, C. R. Schwichtenberg, K. W. Dennis, R. W. McCallum, and D. C. Jiles, "Metal-bonded Co-ferrite composites for magnetostrictive torque sensor applications," *IEEE Trans. Magn.*, vol. 35, no. 5, pp. 3652–3654, Sep. 1999.

[13] B. D. Cullity and C. D. Graham, "Magnetostriction and the effects of stress," in *Introduction to Magnetic Materials*, 2nd ed. Hoboken, NJ, USA: Wiley, 2009, ch. 8, p. 251.

[14] A. E. Clark, M. Wun-Fogle, J. B. Restorff, K. W. Dennis, T. A. Lograsso, and R. W. McCallum, "Temperature dependence of the magnetic anisotropy and magnetostriction of $Fe_{100-x}Ga_x$ (x=8.6, 16.6, 28.5)," *J. Appl. Phys.*, vol. 97, no. 10, May 2005, Art. no. 10M316.

[15] E. C. Estrine, M. Hein, W. P. Robbins, and B. J. H. Stadler, "Composition and crystallinity in electrochemically deposited magnetostrictive galfenol (FeGa)," *J. Appl. Phys.*, vol. 115, no. 17, May 2014, Art. no. 17A918.

[16] Z. Yang, Z. He, D. Li, and C. Rong, "Bias magnetic field of stack giant magnetostrictive actuator: design, analysis, and optimization," *Adv. Mater. Sci. Eng.*, vol. 2016, Art. no. 1704594. Accessed: Feb. 11, 2018. [Online]. Available: https://www.hindawi.com/journals/amse/2016/1704594/

[17] G. Raghunath and A. B. Flatau, "Wireless magneto-elastic torque sensor system," presented at 52nd Aerosp. Sci. Meeting, AIAA SciTech Forum, Jan. 2014. doi: 10.2514/6.2014-0005.

[18] Z. Deng and M. J. Dapino, "Magnetic flux biasing of magnetostrictive sensors," *Smart Mater. Struct.*, vol. 26, no. 5, May 2017, Art. no. 055027.

[19] T. P. Nolan, R. Sinclair, R. Ranjan, and T. Yamashita, "Microstructure and crystallography of textured CoCrTa/Cr recording media," *Ultramicroscopy*, vol. 47, no. 4, pp. 437–446, Dec. 1992.

[20] P. D. McGary and B. J. H. Stadler, "Electrochemical deposition of $Fe_{1-x}Ga_x$ nanowire arrays," *J. Appl. Phys.*, vol. 97, no. 10, May 2005, Art. no. 10R503.

[21] S. M. Reddy, J. J. Park, S.-M. Na, M. M. Maqableh, A. B. Flatau, and B. J. H. Stadler, "Electrochemical synthesis of magnetostrictive Fe–Ga/Cu multilayered nanowire arrays with tailored magnetic response," *Adv. Funct. Mater.*, vol. 21, no. 24, pp. 4677–4683, Dec. 2011.

[22] N. Lupu, H. Chiriac, and P. Pascariu, "Electrochemical deposition of FeGa/NiFe magnetic multilayered films and nanowire arrays," *J. Appl. Phys.*, vol. 103, no. 7, Apr. 2008, Art. no. 07B511.

[23] D. R. Gabe and F. C. Walsh, "The rotating cylinder electrode: A review of development," *J. Appl. Electrochem.*, vol. 13, no. 1, pp. 3–22, 1983.

[24] D. R. Gabe, "The rotating cylinder electrode," *J. Appl. Electrochem.*, vol. 4, no. 2, pp. 91–108, 1974.

[25] D. R. Gabe, G. D. Wilcox, J. Gonzalez-Garcia, and F. C. Walsh, "The rotating cylinder electrode: Its continued development and application," *J. Appl. Electrochem.*, vol. 28, no. 8, pp. 759–780, 1998.
[26] C. T. J. Low, C. Ponce de Leon, and F. C. Walsh, "The rotating cylinder electrode (RCE) and its application to the electrodeposition of metals," *Austral. J. Chem.*, vol. 58, no. 4, pp. 246–262, Jul. 2005.
[27] E. C. Estrine, W. P. Robbins, M. M. Maqableh, and B. J. H. Stadler, "Electrodeposition and characterization of magnetostrictive galfenol (FeGa) thin films for use in microelectromechanical systems," *J. Appl. Phys.*, vol. 113, no. 17, Jan. 2013, Art. no. 17A937.
[28] J. M. Gere and B. J. Goodno, "Stress and Strain in Pure Shear," in *Mechanics of Materials*, vol. 5, 7th ed. Toronto, ON, Canada: Cengage Learning, 2009, ch. 3, sec. 3, p. 248.
[29] (May 15, 2017). *Wikiversity Contributors*. circle.https://en.wikiversity.org/w/index.php?title=Mohr%27s_circle&oldid=1681523
[30] B. R. Muller, "Characterizing the quasi-static and dynamic response of a non-contact magneto-elastic torque sensor," M.S. thesis, Dept. Aerosp. Eng., Univ. Maryland, College Park, MD, USA Maryland, 2017.

Matt Hein received the B.S. degree in biomedical engineering from the University of Minnesota Twin Cities, Minneapolis, MN, USA, in 2010, where he is currently pursuing the Ph.D. degree in electrical engineering.

Since 2009, he has been involved in several projects integrating magnetics technology into biomedical applications both academically and industrially. He currently works in the Greater Los Angeles area on magnetic sensor applications for a major medical device company. His primary research interest is electromagnetic tracking for biomedical applications where he has multiple patent applications. Other interest includes magnetic sensors technology and other magnetic applications in medicine.

Jungjin Park was born in Seoul, South Korea. He received the B.Eng. degree in metallurgical engineering and materials science, Hongik University, South Korea, and the Ph.D. degree in materials science and engineering from the University of Maryland, MD, USA, in 2007. From 2006 to 2009, he joined the National Institute of Standards and Technology, Gaithersburg, MD, USA, as a Guest Researcher. His research interest was the interaction of nanoparticles with the surrounding biological environment, employing quantum dot nanoparticles. Currently, he is an Assistant Research Scientist with the Department of Aerospace Engineering, University of Maryland, where he is involved in the realization of nano and macro scaled magnetostrictive nanowire for various applications, including pressure sensor and flow sensor.

Joseph A. Cozzo received the B.S. degree in aerospace engineering from the University of Maryland, College Park, Maryland, in 2016. He is currently pursuing the M.S. degree in space systems engineering with Johns Hopkins University, Baltimore, MD, USA.

He was an Undergraduate Research Assistant with the University of Maryland from 2013 to 2016 studying magnetostrictive material applications. Since 2016, he has been a Submarine Navigation Analyst with the Johns Hopkins University Applied Physics Lab, Laurel, MD, USA.

Alison Flatau received the Ph.D. degree in mechanical engineering from the University of Utah. She taught and conducted research with the Aerospace Engineering and Engineering Mechanics Department, Iowa State University, from 1990 to 1998, and served as a Program Manager for the Dynamical Systems Modeling Sensing and Control Program with the National Science Foundation from 1998 to 2002. She was with the National Small Wind Systems Test Center, Rockwell International. She is a Professor and the Associate Chair of the Department of Aerospace Engineering, University of Maryland. She is also an Affiliate Faculty Member with the Materials Science and Engineering Department. She is a Fellow of the AIAA and the ASME.

Bethanie J. H. Stadler (SM'99) is a Professor and an Associate Head of the Electrical and Computer Engineering Department, University of Minnesota Twin Cities. She received the B.S. degree from Case Western Reserve University and the Ph.D. degree from MIT. She is a Fellow of MRS. She served as the Chair for the 2004 Fall MRS Meeting and as the Director, the Secretary, and the Program Development Subcommittee Chair for MRS. She will serve as the Program Committee Chair for the Magnetism and Magnetic Materials Conference in 2020 and as the General Co-Chair for Intermag 2023 in Sendai, Japan. She was a 2015 IEEE Magnetics Society Distinguished Lecturer, taught at the IEEE Magnetic Summer School in India (2012), in Italy (2013), and hosted in Minnesota (2015).